

Electronic Supplementary information

Visualizing transport in thiazole flanked isoindigo-based donor-acceptor polymer field-effect transistors

John Barron^a, Salahuddin Attar^b, Payal Bhattacharya^a, Ping Yu^a, Mohammed Al-Hashimi^{b*}
and Suchismita Guha^{a**}

^aDepartment of Physics and Astronomy, University of Missouri, Columbia, MO 65211, USA

^bDepartment of Chemistry, Texas A&M University at Qatar, P.O. Box 23874, Doha, Qatar

E-mail: *mohammed.al-hashimi@tamu.edu, **guhas@missouri.edu

Contents

1. Synthesis and Device Fabrication.....	2
1.1. Materials and Synthesis	2
1.2. Materials Characterization.....	2
1.3. Organic Thin-Film Transistor Device Fabrication Procedure	2
1.4. Synthetic Procedures	3
1.4.1 Synthesis of (E)-1,1'-bis(4-decyltetradecyl)-7,7'-difluoro-6,6'-di(thiazol-2-yl)-[3,3'-biindolinylidene]-2,2'-dione (2)	3
1.4.2 Synthesis of (E)-6,6'-bis(5-bromothiazol-2-yl)-1,1'-bis(4-decyltetradecyl)-7,7'-difluoro-[3,3'-biindolinylidene]-2,2'-dione (M1).....	4
1.4.3 General Procedure for Polymer Synthesis	5
1.4.4 Table S1. Explored reaction conditions for the Bromination of 3	5
1.4.5 Table S2. Bromination condition for 3 using Pyridine/Bromine mixture.	5
1.5. Thermal and Optical Properties, and NMR Results	6
1.5.1 Concentration Dependent UV-Vis.....	6
1.5.2 NMR/Mass Spectroscopic Characterization	7
1.6. Crystallinity and Morphology.....	14
1.7. Bottom-gate-top-contact FET Characteristics.....	16
1.8. Other FET Characteristics.....	17
1.9. EFISHG Experimental Setup and Other Results from P2 FETs	19
1.9.1 Setup and Third Harmonic Generation.....	19
1.9.2 TR-EFISHG Results from Aged P2 FETs.....	20
1.9.3 TR-EFISHG Results from a high mol. wt P2 FET.....	20

1. Synthesis and Device Fabrication

1.1. Materials and Synthesis

All commercially available solvents were distilled and freshly dried by standard drying methods. Reagents and chemicals were used as received without further purification unless otherwise stated. All chemicals were purchased from Solarmer Inc. (E)-6,6'-dibromo-1,1'-bis(4-decyltetradecyl)-7,7'-difluoro-[3,3'-biindolylidene]-2,2'-dione (**1**) were purchased from Solarmer Inc. 2-tributylstannyl thiazole (**2**) was prepared according to reported procedure.¹ Unless otherwise stated, all operations and reactions were carried out under argon using standard Schlenk line techniques. Analytical thin-layer chromatography was performed on Merck aluminum-backed plates pre-coated with silica (0.2 mm, 60 F254) gel. Plates were visualized by exposure to UV light (254 nm) or (365 nm). Flash chromatography (FC) was performed on silica gel (Merck Kieselgel 60 F254 230-400 mesh).

1.2. Materials Characterization

¹H and ¹³C NMR spectra were recorded on a Bruker AV-400 (400 MHz or 600 MHz), using the residual solvent resonance of CDCl₃ or TMS as an internal reference and are given in ppm. Number-average (M_n) and weight average (M_w) were determined by Agilent Technologies 1200 series GPC running in chlorobenzene at 80 °C, using two PL mixed B columns in series, and calibrated against narrow polydispersity polystyrene standards. UV-vis spectra were recorded on a UV- 1601 Shimadzu UV-vis spectrometer. Differential scanning calorimetry (DSC) analysis were recorded on Mettler in nitrogen at 10 °C min⁻¹ of heating rate from 30 °C to 350 °C in two cycles heating-cooling, and thermogravimetric analysis (TGA) curves were collected on Mettler in nitrogen at 10 °C min⁻¹ of heating rate from 30 °C to 600 °C. Cyclic voltammetry (CV) measurements of polymers films were performed under argon atmosphere using a CHI760E Voltammetry analyzer with 0.1 M tetra-n-butylammonium hexafluorophosphate in acetonitrile as the supporting electrolyte. A glassy carbon working electrode, a platinum wire counter electrode, and a silver wire (Ag/AgNO₃) reference electrode were employed, and the ferrocene/ferrocenium (Fc/Fc⁺) was used as the internal reference for all measurements. The scanning rate was 100 mV/s. Polymer films were drop-casted from chloroform solutions on a glassy carbon working electrode (2 mm in diameter).

1.3. Organic Thin-Film Transistor Device Fabrication Procedure

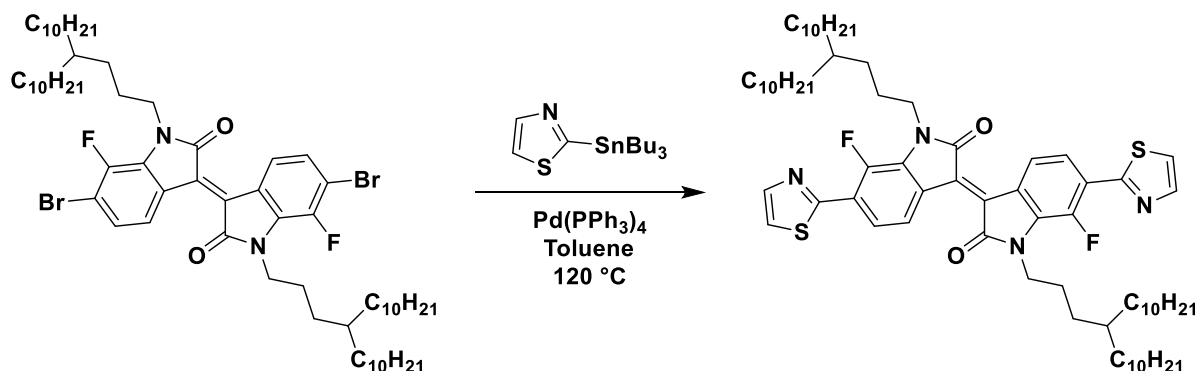
The FETs were fabricated in two different staggered architectures, bottom gate and top contact (BGTC) and top gate and bottom contact (TGBC). The former architecture was made utilizing a silicon substrate with heavily p-doped Si⁺⁺ and a 200 nm SiO₂ oxide layer acting as the dielectric layer. The latter architecture was made using glass as the substrate. Both the silicon and glass were cut into 1" x 1" squares using a diamond-tipped pen and then washed using an organic cleaning method. The substrates were rinsed with acetone and sonicated in an acetone bath for 10 minutes. They were then rinsed with isopropanol and sonicated in an isopropanol bath for 10 minutes. Finally, they were rinsed with DI water, dried with compressed air, and allowed to bake at 100 °C in an oven to remove any trace moisture. The silicon substrates were subsequently cleaned by placing them in a Pirhana solution (using a 10:3 ratio by volume of sulfuric acid to hydrogen peroxide) for 10 minutes. This acts to remove any remaining organic contaminants and makes the surface more hydrophilic. Later, the substrates were placed into a solution of octadecyltrichlorosilane (OTS) (about 25 mg/mL in HPLC-grade toluene) to form a self-assembled monolayer (SAM) on top of the SiO₂ surface, making it more hydrophobic. For the TGBC devices made on glass, 50 nm gold contacts were deposited onto the cleaned glass substrates via thermal evaporation with a patterning mask. This mask was made to give four sets of

source and drain contacts with long strips leading to larger contact pads for probing or soldering wires onto. The contacts themselves had a channel width of 1000 μm and had four different channel lengths, resulting in different W/L ratios: 50 μm , 75 μm , 100 μm , and 125 μm . The gold contacts were subsequently cleaned via an ozone treatment. For the initial set of FETs (those made on silicon), copolymers **P1** and **P2** were dissolved in equal parts of chloroform and dichlorobenzene at a 5 mg/mL concentration. The solution was heated for several hours on a hotplate (up to 150 $^{\circ}\text{C}$) and allowed to stir overnight off heat. The solutions were then filtered through a 0.45 μm PTFE filter. The **P2** copolymer was observed to dissolve better than **P1** and retain most of its volume following filtration. To improve the dissolution of the polymers in the solvent and film formation, dichlorobenzene was used to allow for heating the solution at higher temperatures for the other CYTOP and PMMA devices. The other aspects of the solution (concentration and filtering) were kept the same.

The semiconductor films were formed by spincoating at 1500 RPM for 40 s, with 75 μL of the solution being dynamically cast onto the substrate as it accelerated to its final speed. For the TGBC architecture, the films were restricted to a thin channel by using Teflon tape. The films were then annealed at 180 $^{\circ}\text{C}$ for 10 mins. For the BGTC architecture devices, gold contacts were then thermally evaporated onto the film using a patterning mask to produce many devices with varying W/L ratios. Spincoating and annealing of the semiconductor films were carried out in a glove box under a nitrogen atmosphere. CYTOP solution was made by mixing about 200 μL of CTL-809M with 150 μL of CT-solv-180 to dilute to the desired concentration. To form the dielectric layer for the TGBC devices, the CYTOP solution was spincoated at 2000 RPM for 60 s, placing about 40 μL of solution statically and dynamically casting 100 μL of solution as the substrate accelerated. The film was then annealed at 140 $^{\circ}\text{C}$ for 1.5 hours resulting in a film about 280 nm thick. The PMMA solution was made by dissolving in DMSO at a concentration of 60 mg/mL, which was then heated at 80 $^{\circ}\text{C}$ and magnetically stirred for 45 minutes. The solution was further allowed to stir overnight off heat. The thin film was again formed via spincoating at 5000 RPM for 60 s, with 100 μL being dropped dynamically as the substrate began to accelerate. The PMMA film was then annealed at 100 $^{\circ}\text{C}$ for 20 minutes, resulting in a film about 140 nm thick. When using either CYTOP or PMMA films as the dielectric layer, both were also patterned into a thin channel using Teflon tape while spin coating. Spin coating and annealing of the dielectric films were carried out in a glove box under a nitrogen atmosphere. For the TGBC device, a 50 nm-thick aluminum gate electrode was formed via thermal evaporation. To reduce parasitic currents through the dielectric, a mask was used to pattern the aluminum into a 500 μm -wide channel which was parallel to those formed with the semiconductor and dielectric layers.

1.4. Synthetic Procedures

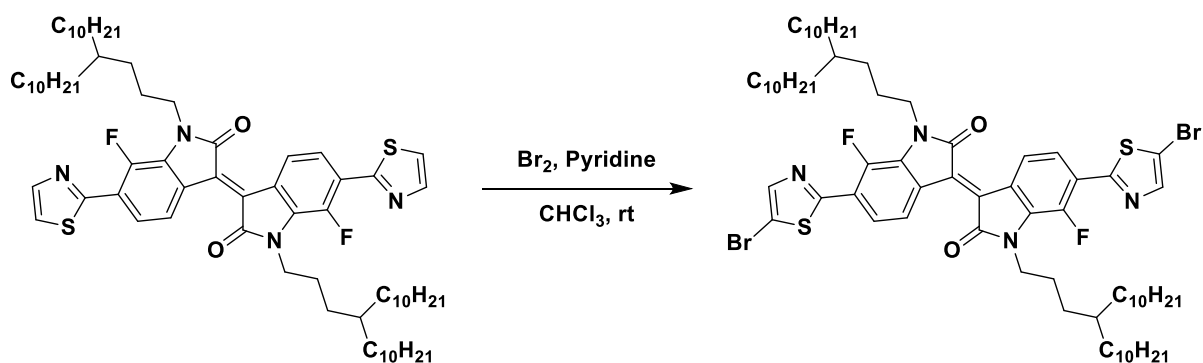
1.4.1 Synthesis of (E)-1,1'-bis(4-decyltetradecyl)-7,7'-difluoro-6,6'-di(thiazol-2-yl)-[3,3'-biindolinylidene]-2,2'-dione (2)



A mixture of (E)-6,6'-dibromo-1,1'-bis(4-decyltetradecyl)-7,7'-difluoro-[3,3'-biindolinylidene]-2,2'-dione **1** (250 mg, 0.221 mmol), 2-(tributylstannyl)thiazole (207 mg, 0.553 mmol) and

Tetrakis(triphenylphosphine)palladium(0) (12.8 mg, 0.011 mmol) was sealed and deoxygenated with argon for 15 min. Toluene (1.5 mL) was added and argon was further purged for 30 mins. The reaction mixture was stirred at 120 °C for 16 h, filtered through Celite and the filtrate was concentrated to dryness to afford a brown solid. Methanol (100 mL) was added and stirred at room temperature for 1 h and filtered to obtain (239 mg, 95 %) of (E)-1,1'-bis(4-decyltetradecyl)-7,7'-difluoro-6,6'-di(thiazol-2-yl)-[3,3'-biindolylidene]-2,2'-dione as dark brown solid. ¹H NMR (400 MHz, CDCl₃) δ 9.09 (d, *J* = 8.6 Hz, 2H), 8.06 – 7.99 (m, 2H), 7.94 (dd, *J* = 8.5, 6.9 Hz, 2H), 7.54 (d, *J* = 3.2 Hz, 2H), 4.01 (t, *J* = 7.1 Hz, 4H), 1.74 (m, 4H), 1.39 – 1.23 (m, 78H), 0.87 (t, *J* = 6.9 Hz, 12H). ¹³C NMR (100 MHz, CDCl₃) δ 167.20, 159.99, 145.51, 143.29, 143.03, 133.28, 132.35, 132.26, 126.13, 125.47, 125.37, 124.80, 121.26, 121.11, 121.03, 42.89, 37.10, 33.55, 31.95, 30.56, 30.16, 29.75, 29.69, 29.39, 26.70, 26.18, 22.71, 14.15. FTMS (APCI, *m/z* of [MH⁺]) Calcd. for [C₇₀H₁₀₆F₂N₄O₂S₂ + H]⁺, *m/z* = 1137.7798. Found: *m/z* = 1137.7816 [M+H]⁺.

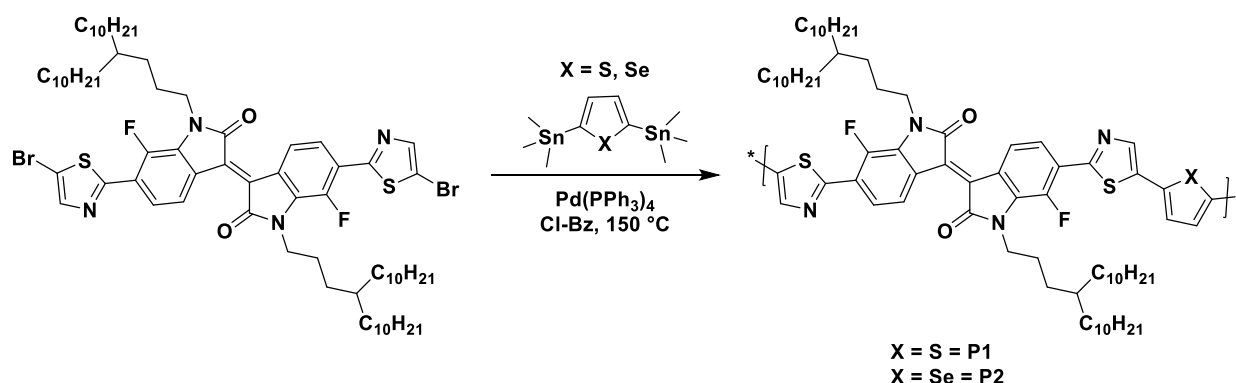
1.4.2 Synthesis of (E)-6,6'-bis(5-bromothiazol-2-yl)-1,1'-bis(4-decyltetradecyl)-7,7'-difluoro-[3,3'-biindolylidene]-2,2'-dione (M1)



To a stirred solution of (E)-1,1'-bis(4-decyltetradecyl)-7,7'-difluoro-6,6'-di(thiazol-2-yl)-[3,3'-biindolylidene]-2,2'-dione (450 mg, 0.39 mmol) and pyridine (127 μL, 1.58 mmol) in chloroform (10 mL) in a light protected flask was added dropwise a solution of bromine (202 μL, 3.95 mmol) in Chloroform (2 mL) at room temperature. The reaction mixture was stirred for 1 h and quenched with saturated sodiumthiosulfate (15 mL), separated organic layer was dried under anhydrous MgSO₄ and concentrated. Column chromatography over silica (30 % Dichloromethane in Hexane) afforded pure (E)-6,6'-bis(5-bromothiazol-2-yl)-1,1'-bis(4-decyltetradecyl)-7,7'-difluoro-[3,3'-biindolylidene]-2,2'-dione (221 mg, 43 %). ¹H NMR (400 MHz, CDCl₃) δ 9.06 (d, *J* = 8.6 Hz, 2H), 7.86 (d, *J* = 2.4 Hz, 2H), 7.85 – 7.79 (m, 1H), 3.97 (t, *J* = 7.2 Hz, 4H), 1.72 (m, 4H), 1.38 – 1.23 (m, 78H), 0.87 (t, *J* = 6.9 Hz, 12H). ¹³C NMR (100 MHz, CDCl₃) δ 166.77, 160.44, 160.39, 144.99, 144.23, 142.52, 132.62, 132.59, 132.09, 132.01, 126.29, 124.77, 124.72, 124.47, 124.38, 119.86, 111.70, 111.59, 42.88, 42.83, 37.13, 33.57, 31.97, 30.63, 30.23, 29.82, 29.81, 29.72, 29.42, 26.75, 26.15, 22.73, 14.16. ¹⁹F NMR (370 MHz, CDCl₃) δ -137.49. FTMS (APCI, *m/z* of [MH⁺]) Calcd. for [C₇₀H₁₀₄Br₂F₂N₄O₂S₂ + H]⁺, *m/z* = 1293.6008 Found: *m/z* = 1293.6034 [M+H]⁺

* Monobrominated (4) and tribrominated (5) monomers were also isolated as side products in low yields.

1.4.3 General Procedure for Polymer Synthesis



A mixture of (E)-6,6'-bis(5-bromothiazol-2-yl)-1,1'-bis(4-decyltetradecyl)-7,7'-difluoro-[3,3'-biindolinylidene]-2,2'-dione (125 mg, 0.096 mmol), 2,5-bis(trimethylstannyl)thiophene (39.5 mg, 0.096 mmol) and Tetrakis(triphenylphosphine)palladium(0) (3 mg, 0.002 mmol) was sealed in microwave vial and deoxygenated for 30 mins. Chlorobenzene (1.5 mL) was added and reaction mixture was further purged with argon for 30 mins. The reaction mixture was heated at 150 °C for 24 h, diluted with chlorobenzene (2 mL) and precipitated in acidic methanol. The solid obtained was filtered and subjected to sequential Soxhlet extraction using methanol, acetone, hexane, chloroform for 24 h each and finally with chlorobenzene respectively to obtain (85 mg) polymer **P1**.

Using similar procedure **P2** was obtained in 82 mg.

1.4.4 Table S1. Explored reaction conditions for the Bromination of **3**.

Reagents ^(a)	Solvent	Conditions	Result (by TLC)
NBS	CHCl ₃	a) Rt 16h	a) No conversion
		b) Reflux 16h	b) Mono bromo <2 %
NBS	DMF	a) Rt	a) No conversion
		b) 70 °C	b) No Conversion
DMDBH	CHCl ₃	Reflux	Mono Bromo ~5 %
Br ₂	CHCl ₃	Reflux	Mono Bromo <10 %
Br ₂ . Pyridine	CHCl ₃	Rt	Complete conversion with brominated products

^(a) 2.5 Equivalents of reagents

1.4.5 Table S2. Bromination condition for **3** using Pyridine/Bromine mixture.

Pyridine (Eq.)	Br ₂ (Eq.)	Mono	Dibromo	Tribromo
2	2	Major	Very low	no
4	6	Major	Minor	Very low
4	8	Minor	Major	low
4	12	Very low	Major	Major

1.5. Thermal and Optical Properties, and NMR Results

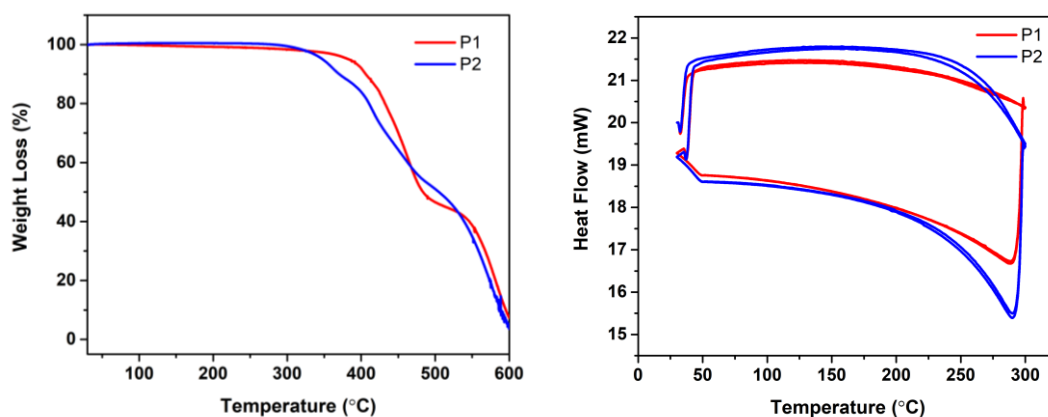


Figure S1. (a) TGA thermograms of polymers **P1** and **P2** under nitrogen flow at $10\text{ }^{\circ}\text{C min}^{-1}$ of heating from $30\text{ }^{\circ}\text{C}$ to $600\text{ }^{\circ}\text{C}$. (b) DSC thermograms of heat scanning for two heating and cooling cycles from $30\text{ }^{\circ}\text{C}$ to $300\text{ }^{\circ}\text{C}$ at $10\text{ }^{\circ}\text{C min}^{-1}$ under nitrogen flow.

1.5.1 Concentration Dependent UV-Vis

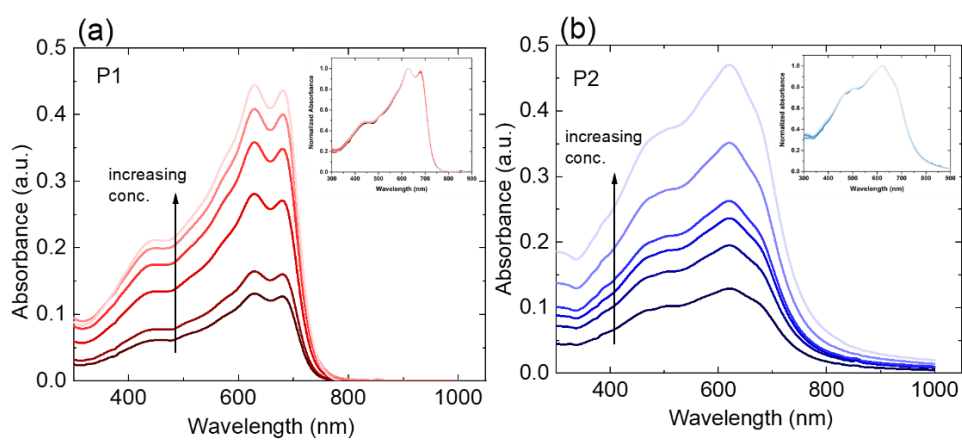
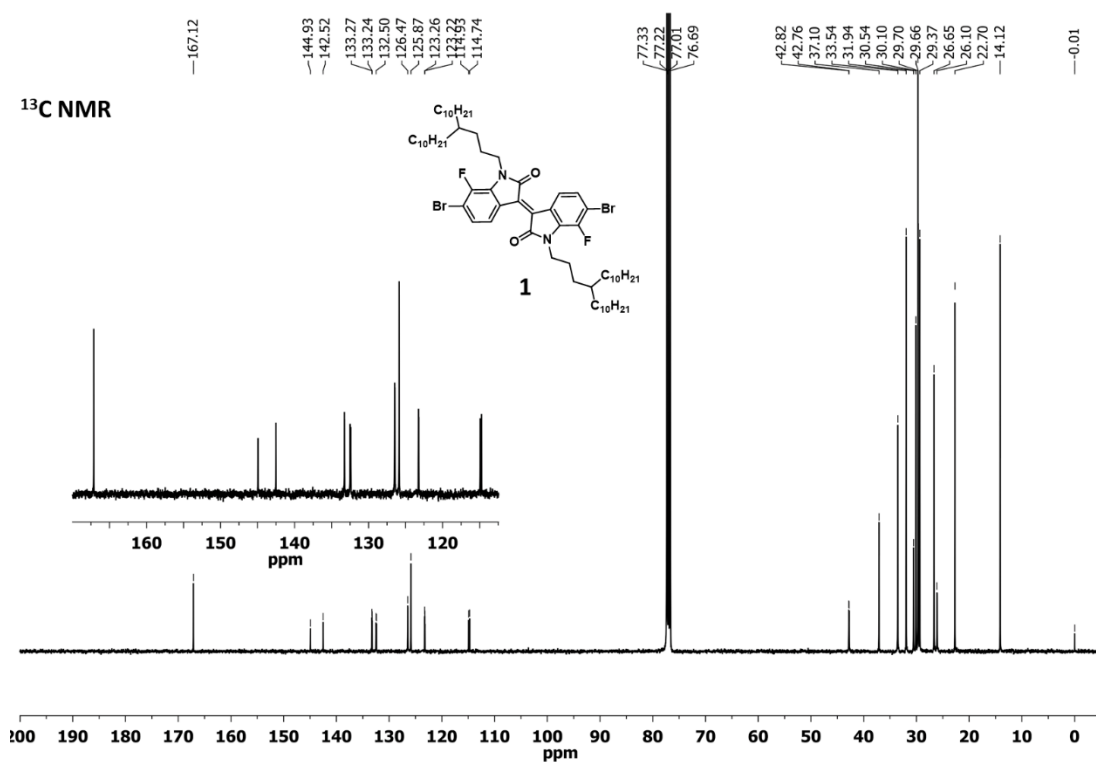
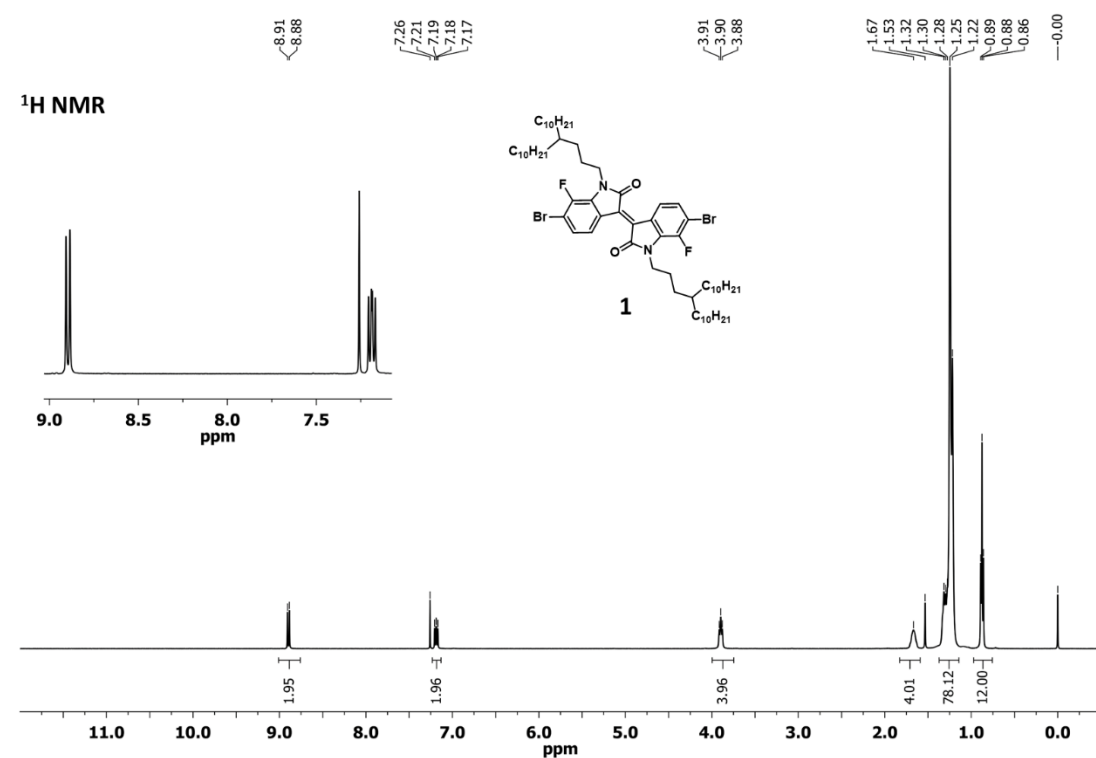
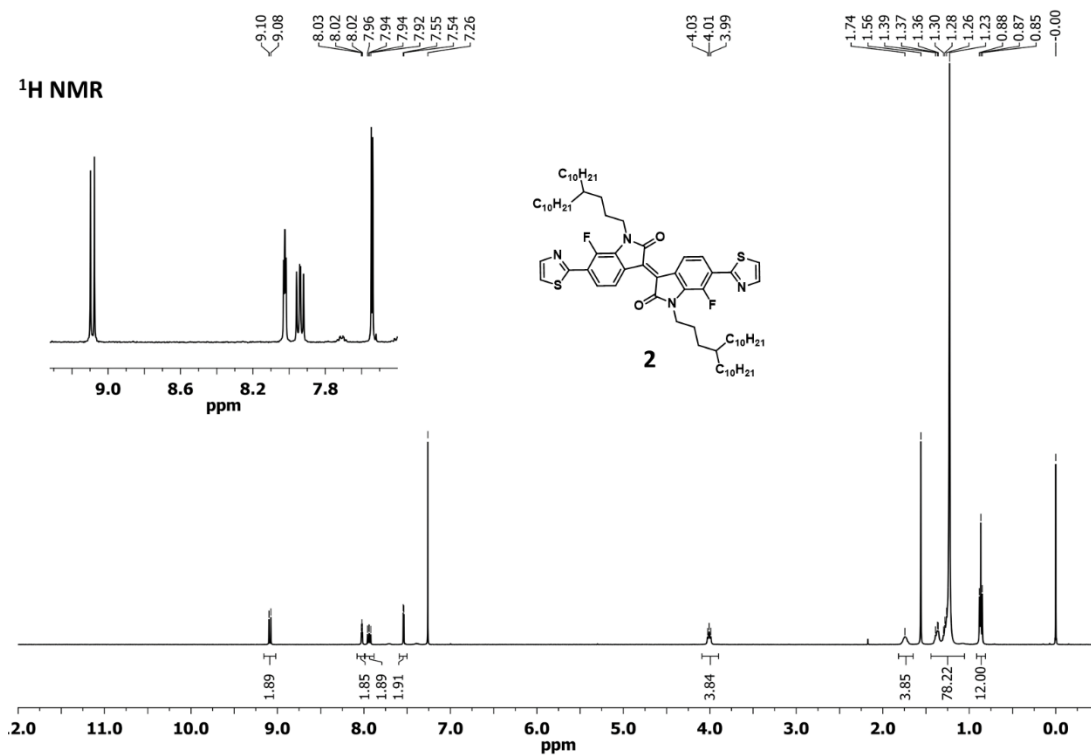


Figure S2. Absorption spectra at different concentrations for **P1** (a) and **P2** (b). The insets show the normalized spectra indicating no change in the absorption features as a function of concentration.

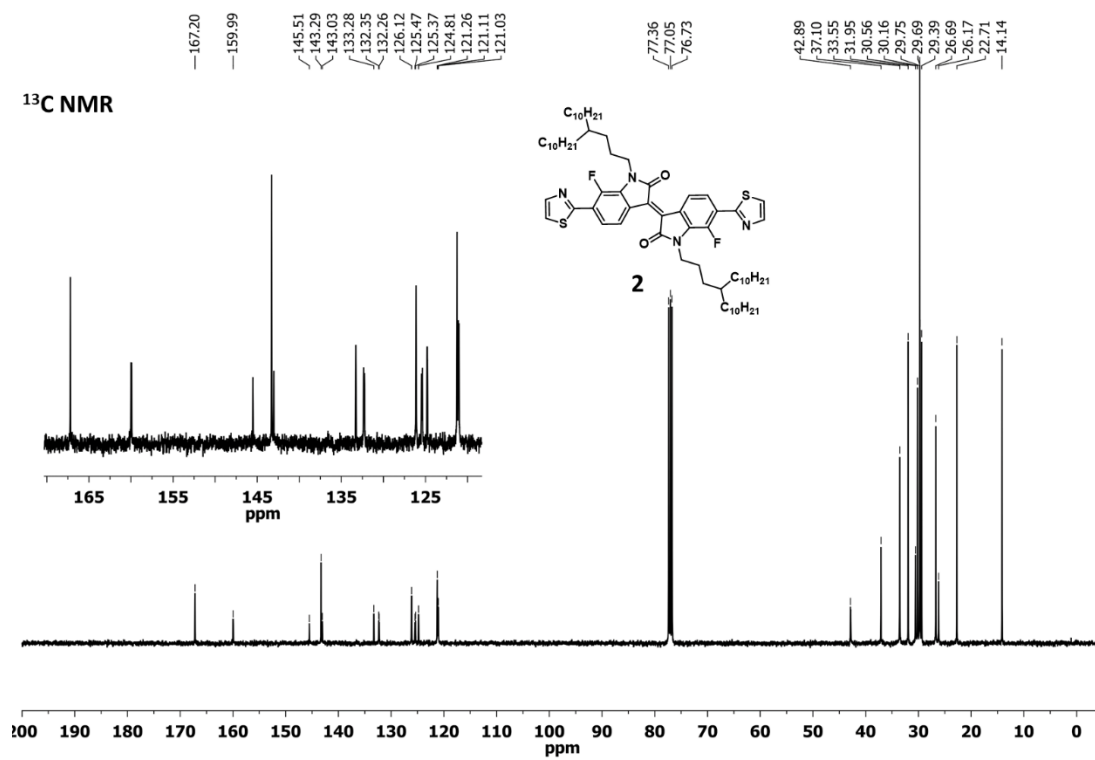
1.5.2 NMR/Mass Spectroscopic Characterization

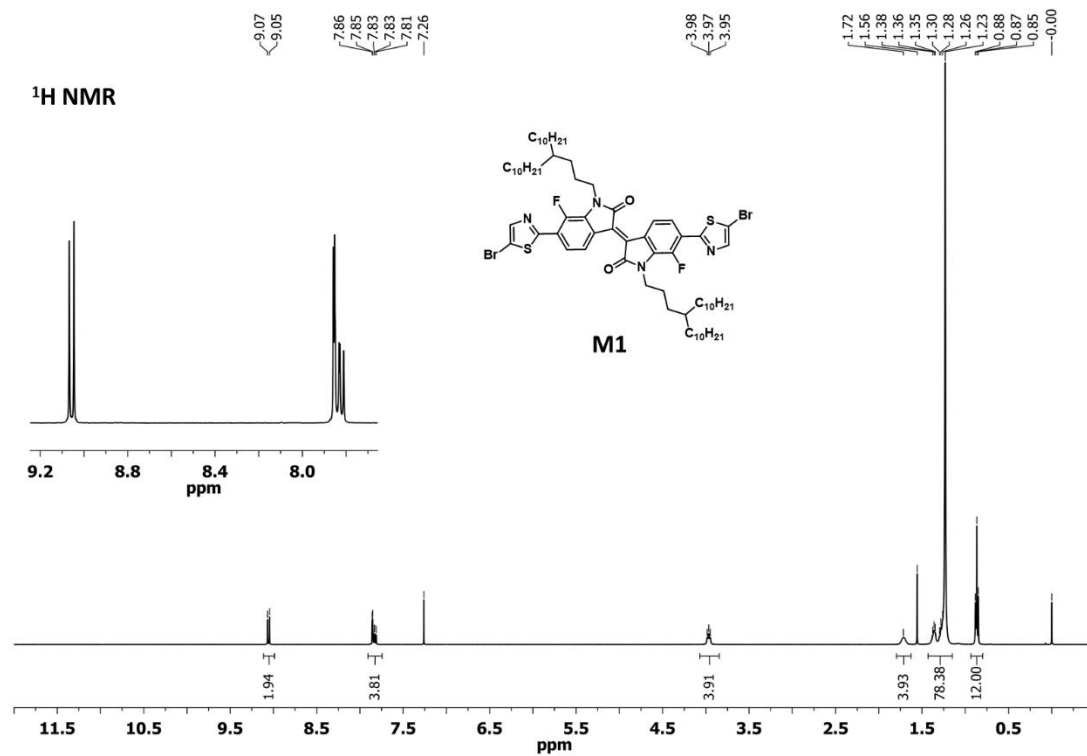
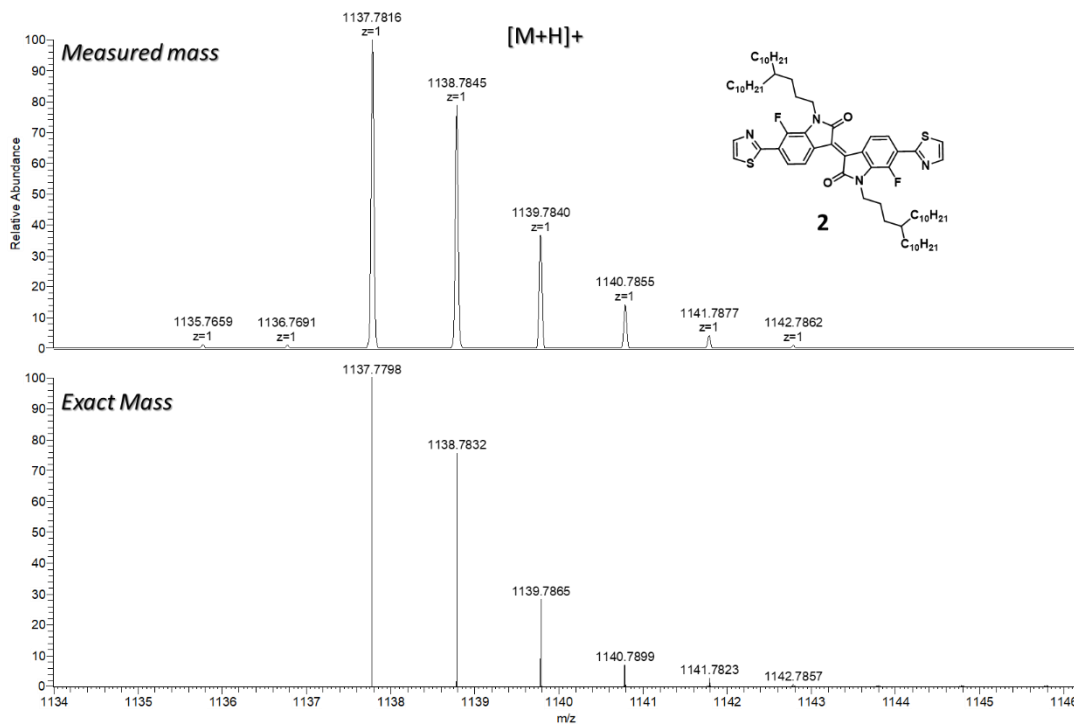


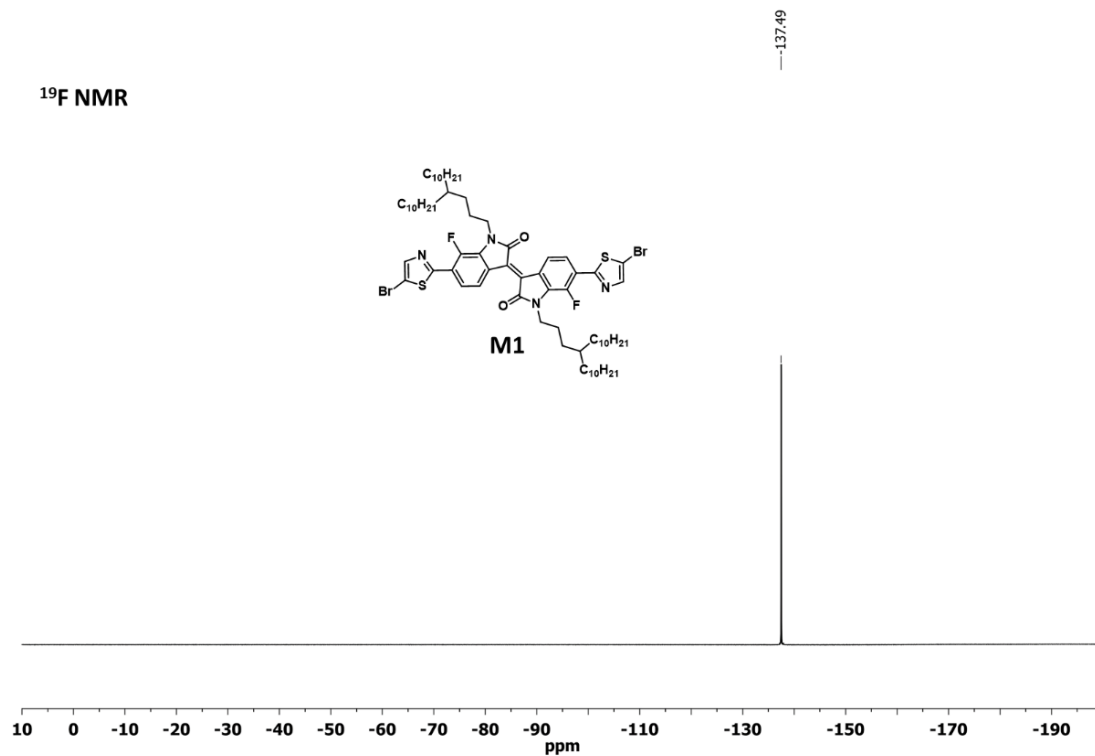
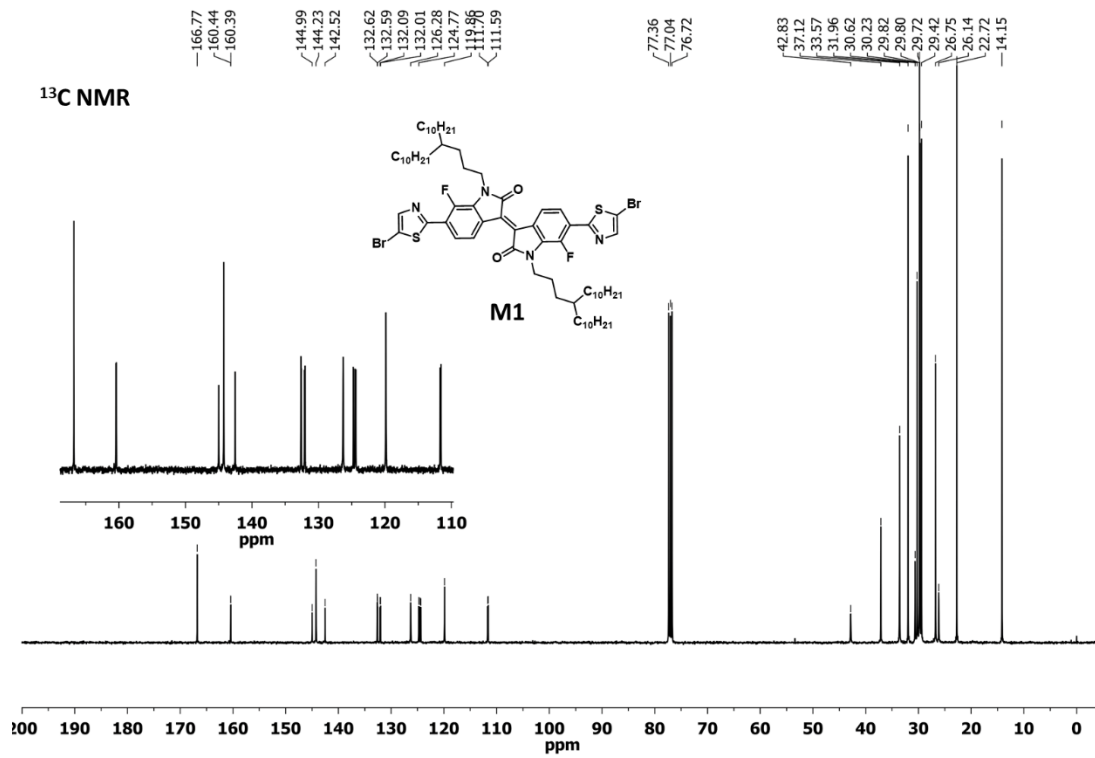
¹H NMR

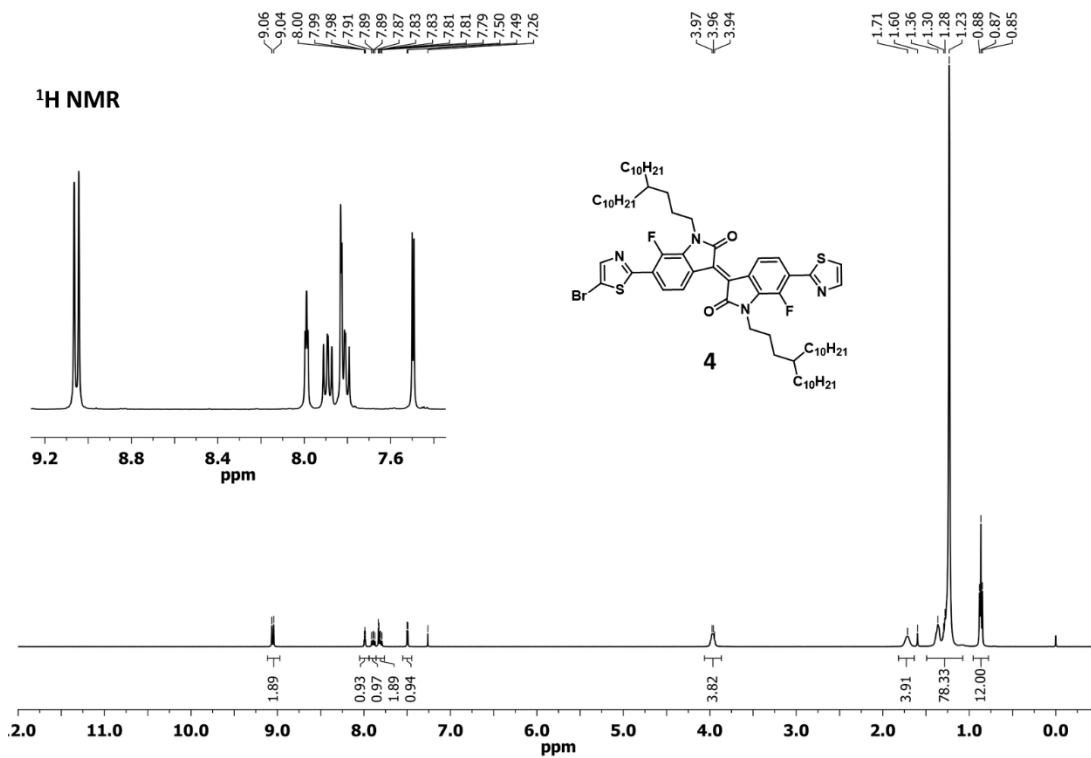
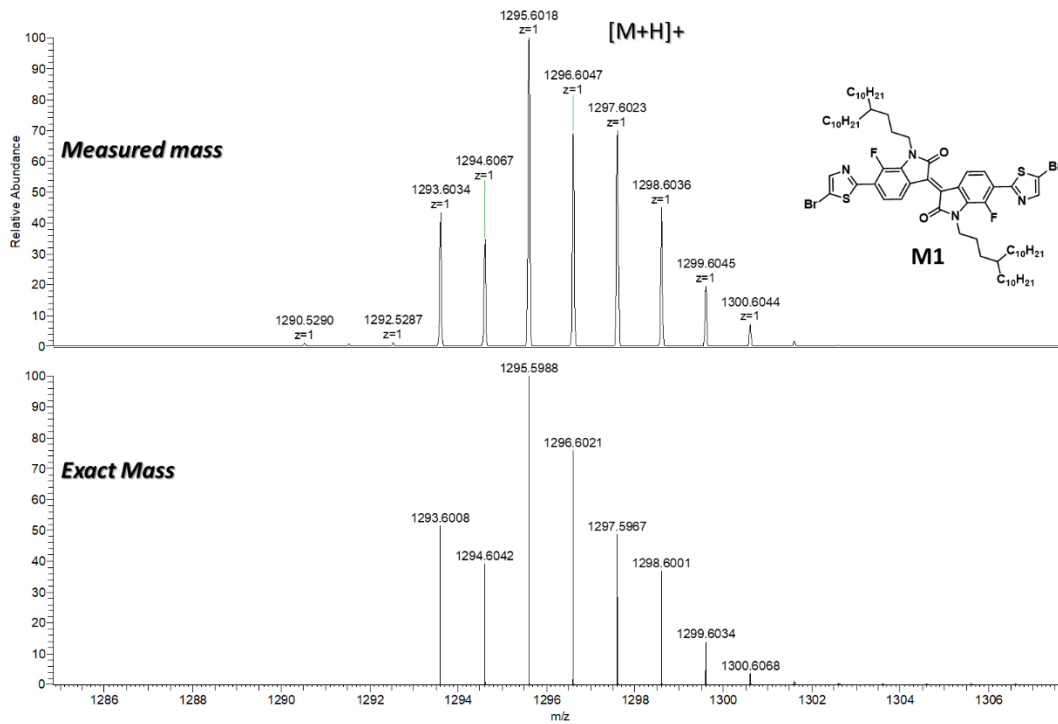


¹³C NMR

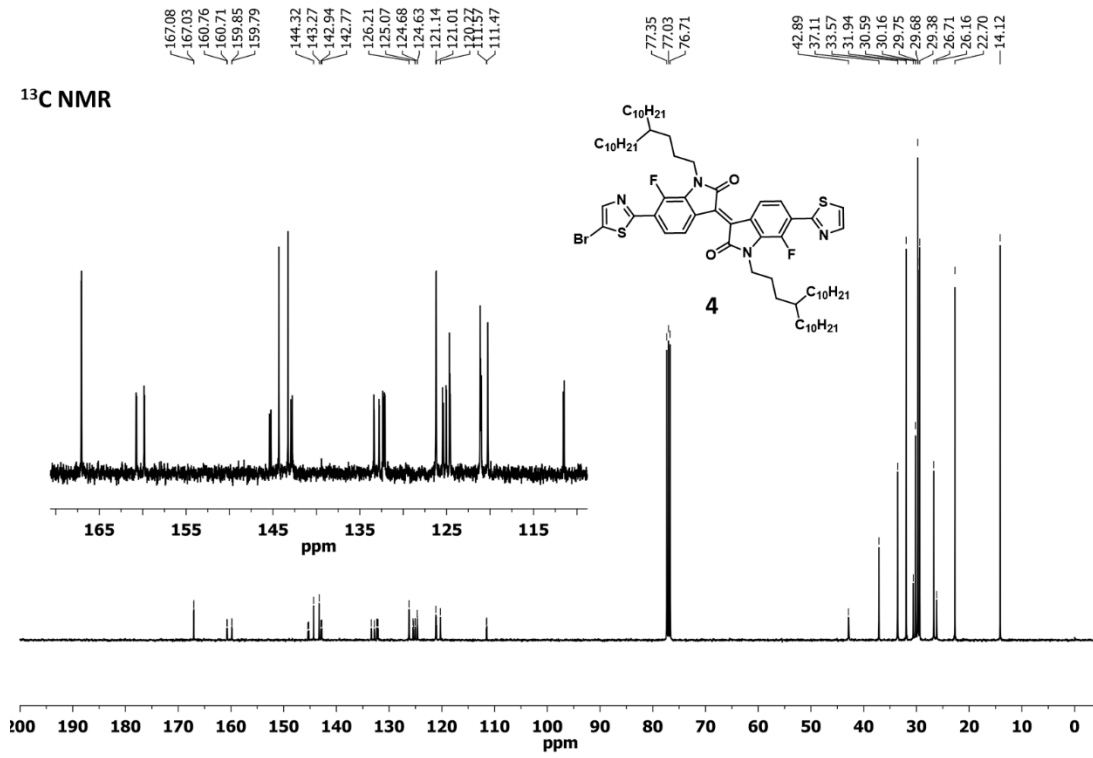


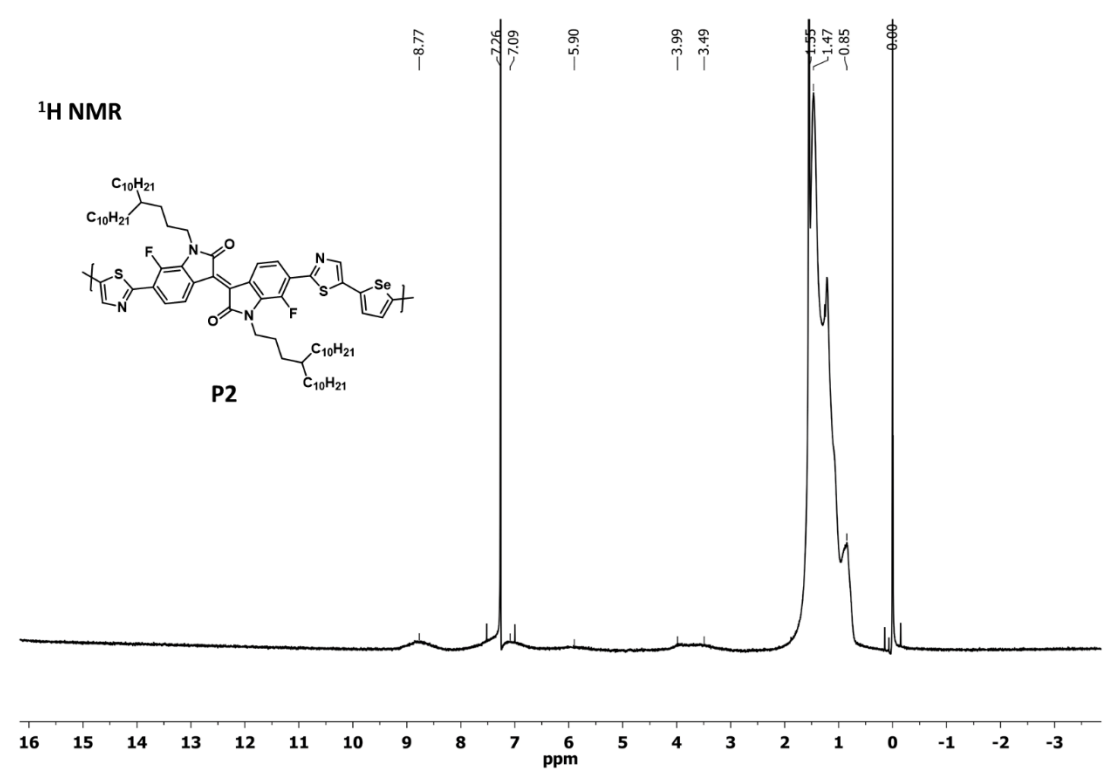
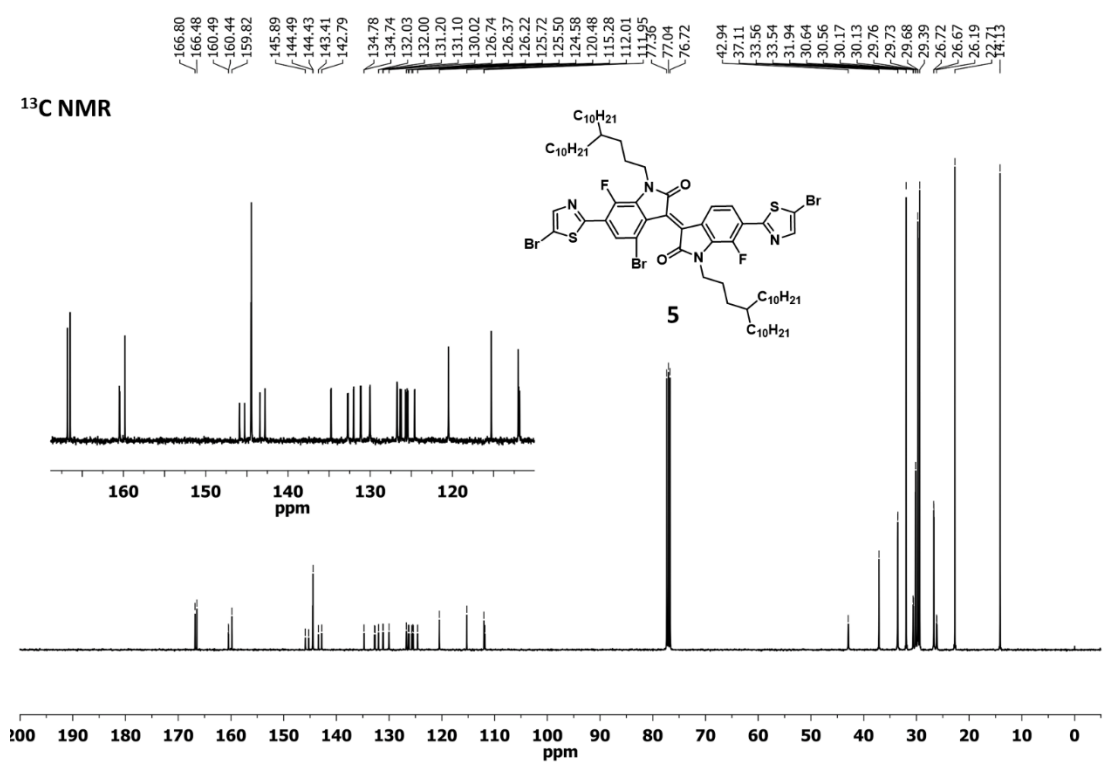






¹³C NMR





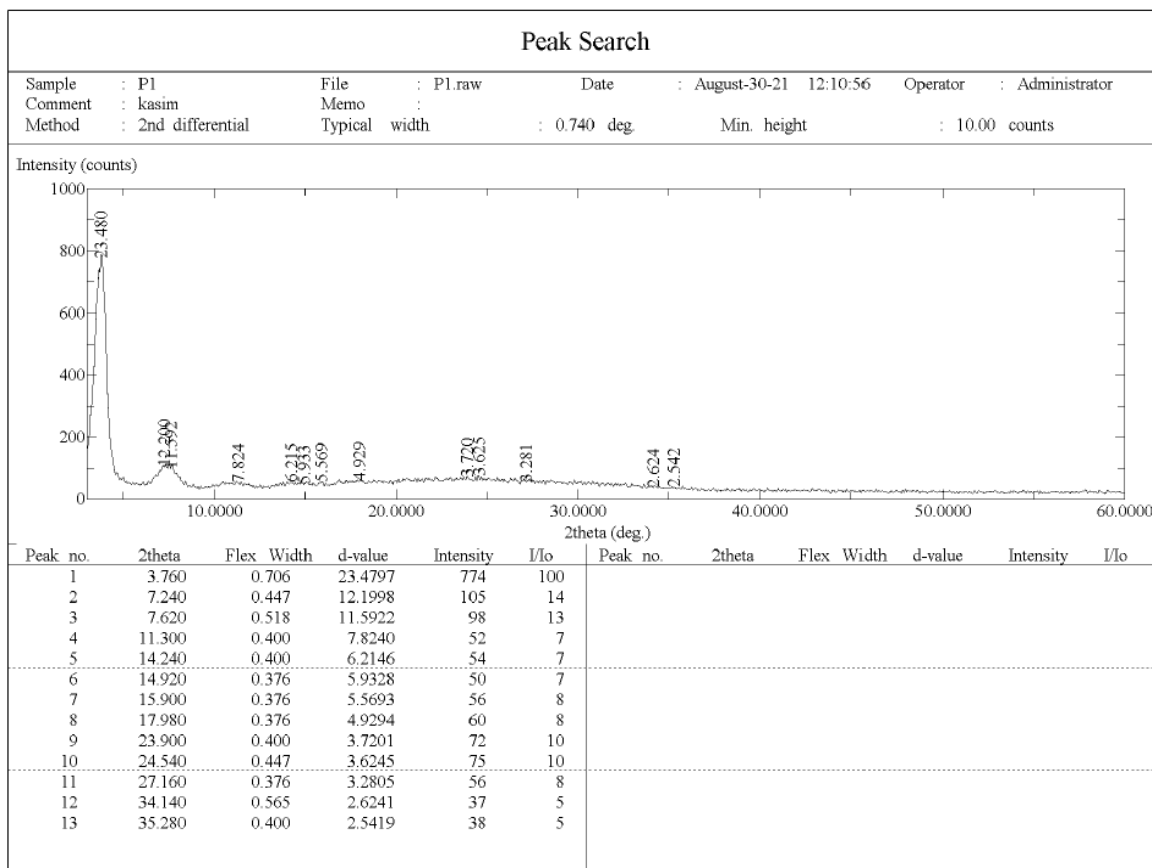
1.6. Crystallinity and Morphology

Thin films of polymers **P1-P2** were fabricated and measured using XRD in order to analyze the relationship between the chemical structure of the polymers and their crystalline behavior. The lamellar/ π - π stacking d-spacing values are summarized in **Table 1**. Details of how these parameters were obtained is as follows:

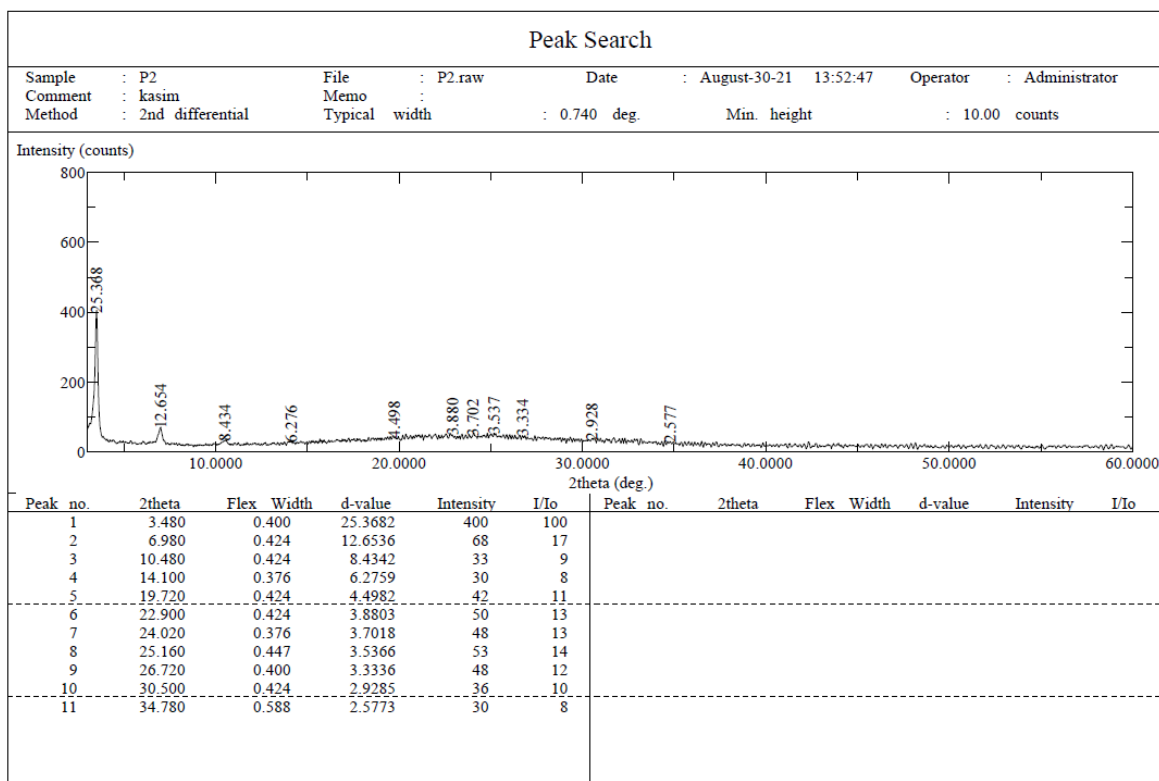
- Mn was determined by GPC (against polystyrene standards) in chlorobenzene at 85 °C
- $\lambda_{\max}^{\text{sol}}$ was in chlorobenzene solution.
- $\lambda_{\max}^{\text{film}}$ was spin-coated from chlorobenzene solution onto a glass surface.
- $E_{\text{HOMO}}/E_{\text{LUMO}} = [-(E_{\text{onset}} - E_{\text{onset}}(\text{FC}/\text{FC}^+ \text{ vs Ag}/\text{Ag}^+)) - 4.8]$ eV, where 4.8 eV is the energy level of ferrocene below the vacuum level and the formal potential $E_{\text{onset}}(\text{FC}/\text{FC}^+ \text{ vs Ag}/\text{Ag}^+)$ is equal to 0.45 V.
- Electrochemical bandgap: $E_g^{\text{el}} = E_{\text{ox/onset}} - E_{\text{red/onset}}$
- Optical bandgap: $E_g^{\text{opt}} = 1240/\lambda_{\text{edge}}$
- Calculated by Bragg's Law $d = \lambda/(2\sin\theta)$, where $\lambda = 1.5406 \text{ \AA}$

As depicted in **Fig. S3** all polymers exhibit similar degree of crystallinity with lamellar 2θ peaks in the range 3.7° to 4.6° and π - π stacking peaks ranging from 18° to 24° . **P2** presented a larger lamellar packing distance (25.37 \AA) compared to **P1** (23.47 \AA). In addition, small lamellar reflection at $2\theta = 7.2^\circ$ was observed for **P1** while that of **P2** was seen at $2\theta = 6.9^\circ$. These results may be ascribed to the presence of Se as the heteroatom in **P2**, thus presenting better packing and higher crystallinity compared with **P1**. These results are in good alignment with the solid-state UV-vis absorption data and the FET results.

Additionally, morphological properties in the solid-state thin films for **P1** and **P2** were evaluated using atomic force microscopy (AFM). As shown in the AFM images of **P1** and **P2** (**Fig. S4**), the Se containing polymer presents slightly better homogeneousness, in comparison with **P1**, which exhibits some nonuniform regions on the surface (**Fig. S4 a**). **P1** has a rougher surface value of root mean square (RMS) roughness of 4.33 nm, while **P2** showed slightly lower value 3.36 nm. In addition, **P1** presents bigger grain sizes as depicted in the phase image of **Fig. S4b**, in comparison with **P2**. These small differences were easily detected by the 3D-height topography as shown in **Fig. S4c** (represented by the same scale for the polymers).



June-20-2022 09:15:27 Page-5



June-20-2022 09:27:52 Page-6

Figure S3. XRD patterns obtained with peaks estimated for P1 (above) and P2 (below).

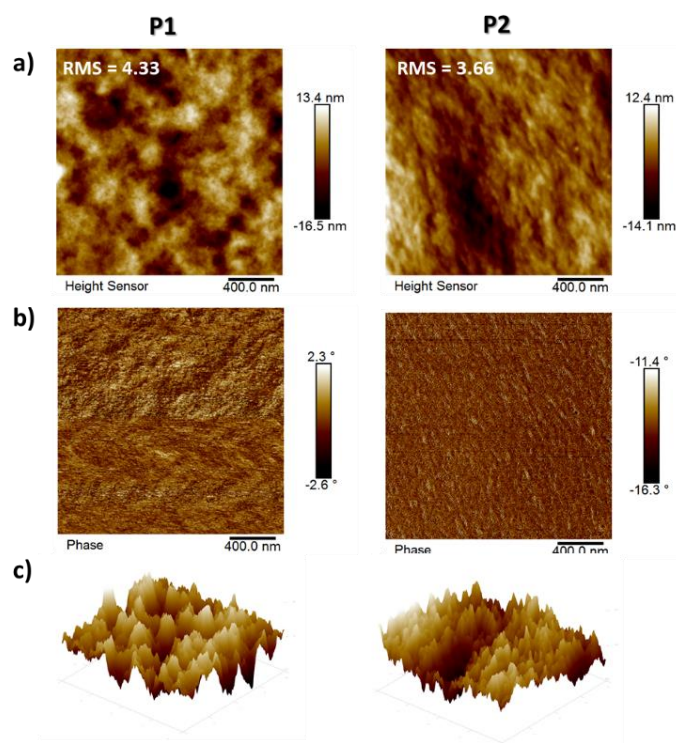


Figure S4. Tapping-mode AFM images of (a) height, (b) phase in $0.4\mu\text{m} \times 0.4\mu\text{m}$ scan size and (c) 3D-topography of polymers P1 and P2

1.7. Bottom-gate-top-contact FET Characteristics

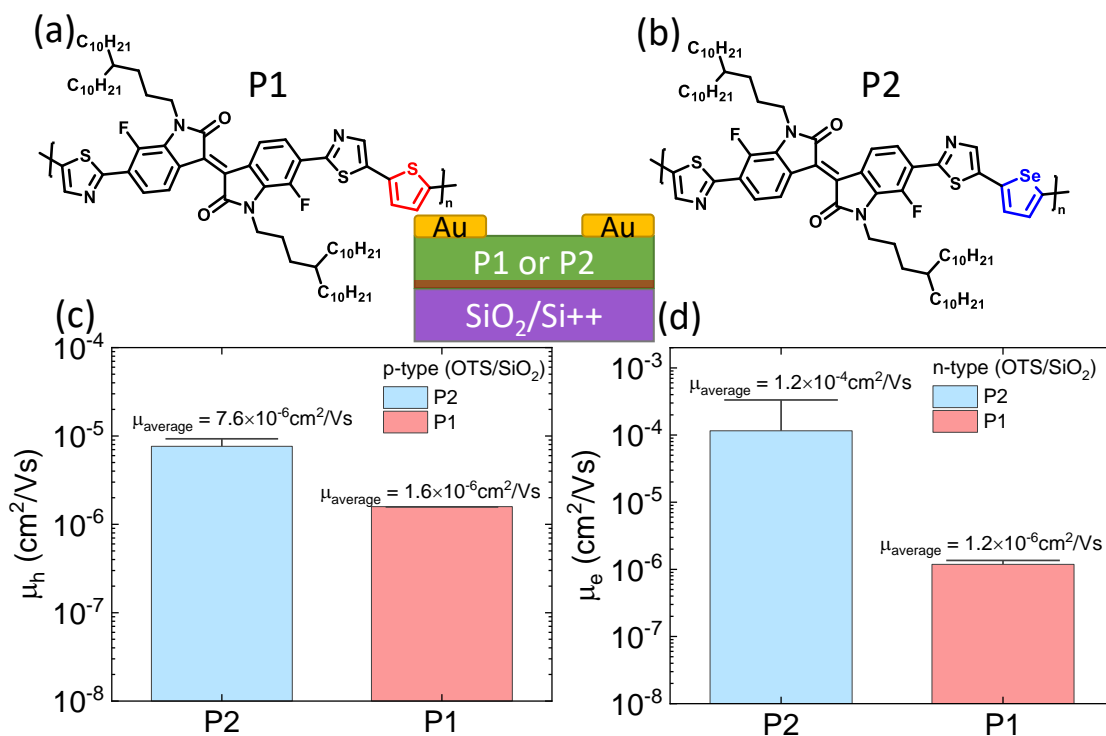


Figure S5. (a) and (b) Chemical structures of **P1** and **P2**. The inset shows the FET architecture where the SiO₂ layer was treated with OTS. (c) The average hole carrier mobilities extracted from the

saturation region of **P1** and **P2** based FETs. (d) The average electron carrier mobilities extracted from the saturation region of **P1** and **P2** based FETs. The average carrier mobilities are obtained from 5-10 devices.

1.8. Other FET Characteristics

Top gate FETs (**P1**)

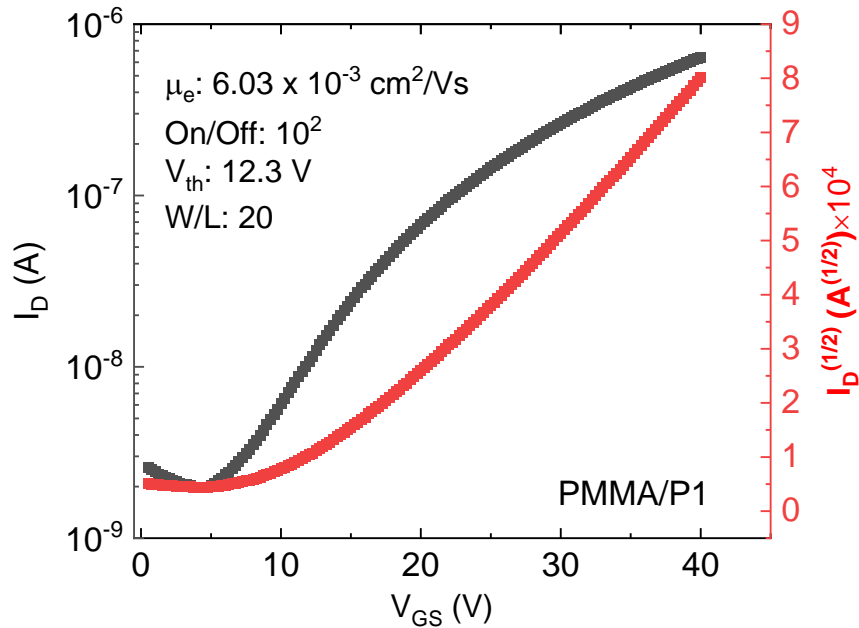


Figure S6. Transfer characteristics from a TGBC PMMA/**P1** FET.

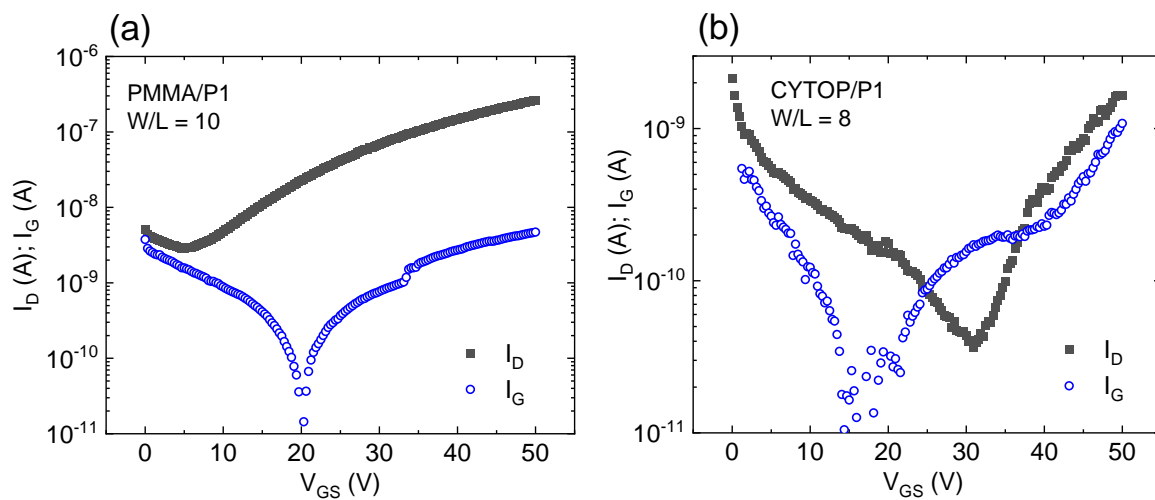


Figure S7. Typical transfer characteristics from TGBC **P1** FETs with gate leakage current in (a) PMMA and (b) CYTOP devices.

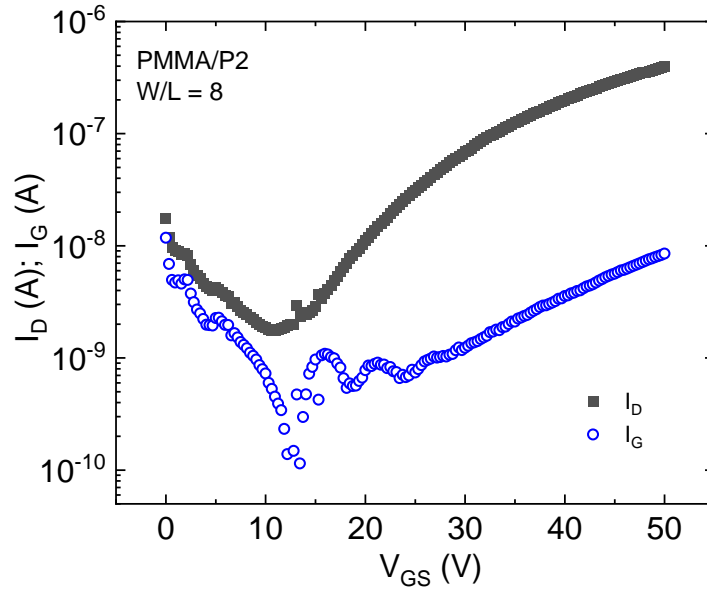


Figure S8. Representative transfer characteristics from a PMMA/P2 FET showing the gate-leakage current.

Linear region characteristics from PMMA/P1 FET:

The saturation regime mobility was calculated from $\mu_{sat} = \frac{2}{c_i} \frac{L}{W} \left(\frac{\partial \sqrt{I_D}}{\partial V_G} \right)^2$ and the linear regime mobilities were calculated from $\mu_{lin} = \frac{L}{c_i W V_{DS}} \frac{\partial I_D}{\partial V_G}$.

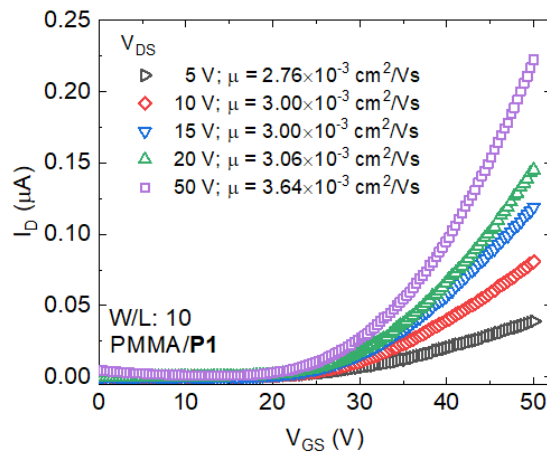


Figure S9. Representative transfer characteristics from a PMMA/P1 FET showing the linear and saturation region. The inset lists the carrier mobilities in the linear region (where V_{DS} varies between 5 V and 20 V) and the saturation region ($V_{DS} = 50$ V).

1.9. EFISHG Experimental Setup and Other Results from P2 FETs

1.9.1 Setup and Third Harmonic Generation

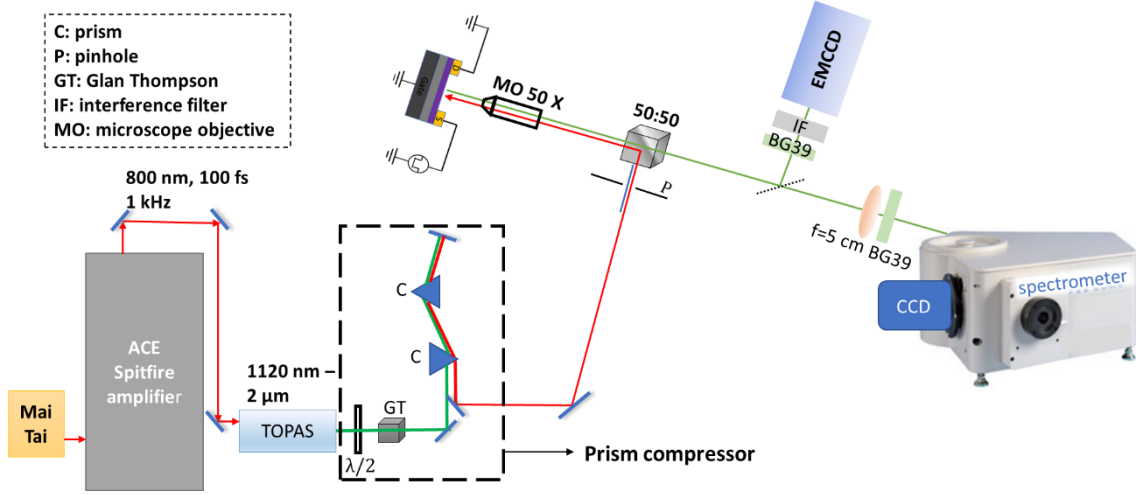


Figure S10. A schematic of the experimental setup.

In EFISHG, the centrosymmetry is broken by the application of an electric field. The induced polarization is given by:

$$P_i^{2\omega} = \chi_{ijkl}^{(3)}(-2\omega; \omega, \omega, 0) E_j^\omega E_k^\omega E_l^0, \quad (1)$$

where E_l^0 is the applied field and $E_j^\omega E_k^\omega$ represent the laser field. $\chi_{ijkl}^{(3)}$ is the third order nonlinear optical susceptibility. Eq. (1) is often written as:

$$P_i^{2\omega} = \chi_{ijk}^{(2)}(-2\omega; \omega, \omega)(E^0) E_j^\omega E_k^\omega, \quad (2)$$

$$\text{with } \chi_{ijk}^{(2)}(-2\omega; \omega, \omega)(E^0) = \chi_{ijkl}^{(3)}(-2\omega; \omega, \omega, 0) E_l^0.$$

The third harmonic (TH) generation was measured from a film of P2 as a function of varying incident wavelength.

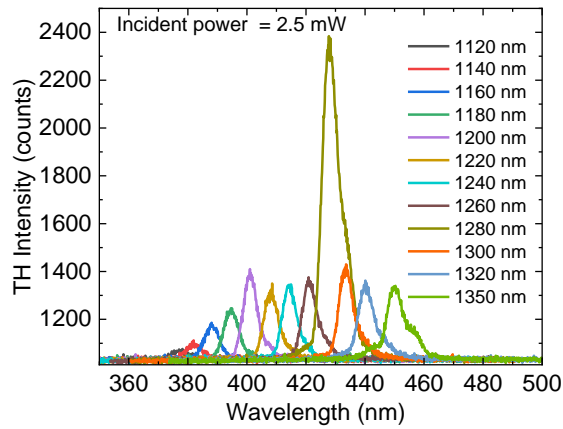


Figure S11. Third harmonic generation from a P2 film as a function of varying incident wavelength. The incident power was the same for each wavelength. A clear resonance is seen when the wavelength = 1280 nm

1.9.2 TR-EFISHG Results from Aged P2 FETs

We have performed TR-EFISHG experiments and acquired images from an aged P2 FET (5 months old) where the overall performance had decreased. The carrier mobility extracted from the EFISHG images is almost an order of magnitude higher compared with the electrical measurements.

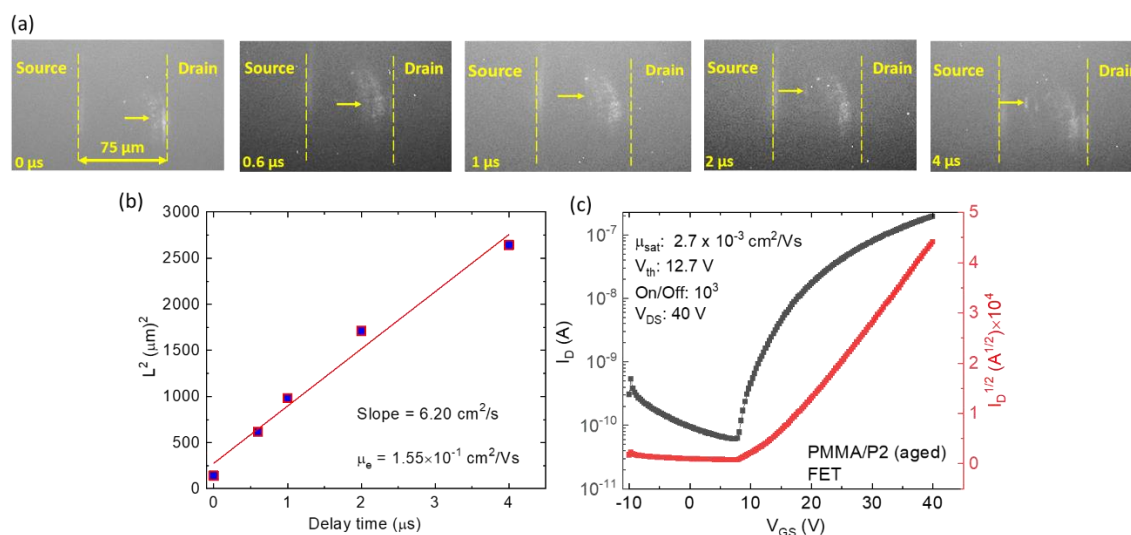


Figure S12. (a) The movement of the EFISHG signal in the channel region of a PMMA/P2 FET with channel length of 75 μm at five different delay times. (b) The position of the carrier front as a function of the delay (transit) time can be described by using eq. (2) (in the manuscript). (c) The transfer characteristics of the same P2 FET.

1.9.3 TR-EFISHG Results from a high mol. wt P2 FET

For the reliability and reproducibility of the TR-EFISHG method, we fabricated P2 FETs with a different mol. wt ($M_n \sim 52$ kDa). These FETs gave an order of magnitude lower carrier mobility (μ_e) from current-voltage characteristics compared with the ones discussed in the manuscript. A TGBC FET with PMMA was used both for electrical and TR-EFISHG methods. TR-EFISHG images from this device for various delay times are shown in Fig. S13. In these images, the drain is on the left and the source is on the right. For this device, $\mu_e(\text{electrical}) = 4.02 \times 10^{-3} \text{ cm}^2/\text{Vs}$ and using the images below, $\mu_e(\text{EFISHG}) = 1.2 \times 10^{-2} \text{ cm}^2/\text{Vs}$.

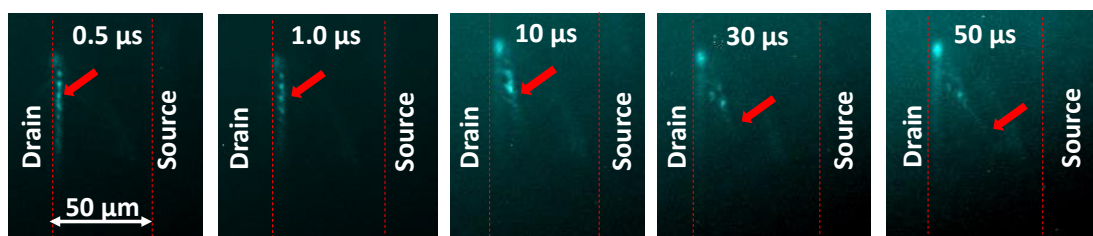


Figure S13. The movement of the EFISHG signal in the channel region of a PMMA/P2 FET (of a different mol. wt) with channel length of 50 μm at five different delay times. Here the drain electrode is on the left and the source is on the right.

References

1. Jang Yong Lee, Kwan Wook Song, Ho Jun Song, Doo Kyung Moon, Synthesis and photovoltaic property of donor–acceptor type conjugated polymer containing carbazole and 4,7-dithiazolylbenzothiadiazole moiety utilized as a promising electron withdrawing unit, *Synthetic Metals*, **161**, 2011, 2434-2440,